Alpha Ketoamides as Broad Spectrum Inhibitors of Coronavirus and Enterovirus Replication: Structure Based Design and Synthesis

Trupti Musne[1], Sangram U. Deshmukh[2], Nandkishor B. Bavage[3], Vidyasagar Galib[4], Shyamlila B. Bavage[5]

[1]*B.Pharmacy Final Year, Latur College of Pharmacy Hasegaon, Tq. Ausa, Dist. Latur-413512, Maharashtra, India*

[2,3]*Department of Pharmaceutical Chemistry, Latur College of Pharmacy Hasegaon, Tq. Ausa, Dist. Latur-413512, Maharashtra, India*

[4]*Department of Pharmaceutical Analysis, Latur College of Pharmacy Hasegaon, Tq. Ausa, Dist. Latur-413512, Maharashtra, India*

[5]*Department of Pharmacognosy, Latur College of Pharmacy, Hasegaon, Tq. Ausa, Dist. Latur-413512, Maharashtra, India*

***Abstract*- Picornaviruses are small non-enveloped RNA viruses with genomic RNA of 7500 – 8000 nucleotides, whereas coronaviruses (CoV) are RNA viruses with larger genome of 27 – 32 kb. Both types of viruses translate their genetic information into polyprotein precursors that are processed by virally encoded 3C proteases (3Cpro) and 3C-like proteases (3CLpro), respectively, to generate functional viral proteins. The main protease of coronaviruses and the 3C protease of enteroviruses share similar active-site architecture and a unique requirement for glutamine in the P1 position of the substrate. Because of their unique specificity and essential role in viral polyprotein processing, these proteases are suitable targets for the development of antiviral drugs.In this review we pursued a structure-based design of peptidomimetic α-ketoamides as inhibitors of main and 3C proteases. Compounds synthesized were tested against the recombinant proteases as well as in viral replicons and virus-infected cell cultures; most of them were not cell-toxic. Optimization of the P2 substituent of the α-ketoamides proved crucial for achieving near-equipotency against the three virus genera. The best near-equipotent inhibitors, 11u and11r display low-micromolar EC50 values against enteroviruses, alpha coronaviruses, and beta coronaviruses in cell cultures. In Huh7 cells, 11r exhibits three-digit picomolar activity against the Middle East Respirator Syndrome coronavirus.**

INTRODUCTION

Seventeen years have passed since the outbreak of severe acute respiratory syndrome (SARS) in 2003, but there is yet no approved treatment for infections with the SARS coronavirus (SARS-CoV). One of the reasons is that, despite the devastating consequences of SARS for the affected patients, the development of an antiviral drug against this virus would not be commercially viable in view of the fact that the virus has been rapidly contained and did not reappear since 2004. As a result, we were empty-handed when the Middle East respiratory syndrome coronavirus (MERS-CoV), a close relative of SARS-CoV, emerged in 2012. MERS is characterized by severe respiratory disease, quite similar to SARS, but in addition, frequently causes renal failure. Although the number of registered MERS cases is low (2494) as of November 30, 2019; the threat MERSCoV poses to global public health may be even more serious than that presented by SARS-CoV. This is related to the high case-fatality rate (about 35%, compared to 10% for SARS) and to the fact that MERS cases are still accumulating seven years after the discovery of the virus, whereas the SARS outbreak was essentially contained within 6 months. The potential for human-to-human transmission of MERS-CoV has been impressively demonstrated by the 2015 outbreak in South Korea, where 186 cases could be traced back to a single infected traveler returning from the Middle East.• SARS-like

coronaviruses are still circulating in bats in China,5−8 from where they may spill over into the human population.

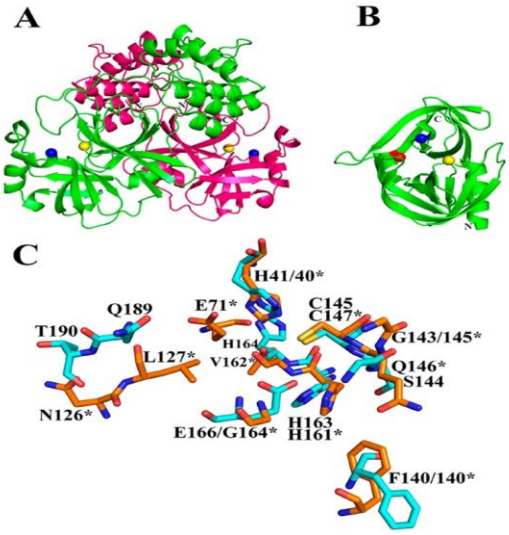

In December 2019, a new coronavirus caused an outbreak of pulmonary disease in the city of Wuhan, the capital of Hubei province in China, and has since spread globally .The virus has been named SARS-CoV-2 .because the RNA genome is about 82% identical to the SARS coronavirus (SARS-CoV); both viruses belong to clade b of the genus Beta coronavirus . The disease caused by SARS-CoV-2 is called COVID-19. Whereas at the beginning of the outbreak, cases were connected to the Huanan seafood and animal market in Wuhan, efficient human-to-human transmission led to exponential growth in the number of cases. On March 11, the World Health Organization (WHO) declared the outbreak a pandemic. As of March 15, there are >170,000 cumulative cases globally, with a ~3.7% case-fatality rate .One of the best characterized drug targets among coronaviruses is the main protease (Mpro, also called 3CLpro) (4).Along with the papain-like protease(s), this enzyme is essential for processing the polyproteins that are translated from the viral RNA . The Mpro operates at no less than 11 cleavage sites on the large polyprotein 1ab (replicase 1ab, ~790kDa); the recognition sequence at most sites is LeuGln↓ (Ser,Ala,Gly) (↓ marks the cleavage site). Inhibiting the activity of this enzyme would block viral replication. Since no human proteases with similar cleavage specificity are known, inhibitors are unlikely to be toxic.

Previously, we designed and synthesized peptidomimetic α-ketoamides as broad-spectrum inhibitors of the main proteases of betacoronaviruses and alphacoronaviruses as well as the 3C proteases of enteroviruses. The best of these compounds showed an EC50 of 400 picomolar against MERS-CoV in Huh7 cells as well as low micromolar EC50 values against SARS-CoV and a whole range of enteroviruses in various cell lines, although the antiviral activity seemed to depend to a great extent on the cell type used in the experiments . In order to improve the half-life of the compound in plasma, we modified 11r by hiding the P3 - P2 amide bond within a pyridone ring, in the expectation that this might prevent cellular proteases from accessing this bond and cleaving it. Further, to increase the solubility of the compound in plasma and to reduce its binding to plasma proteins, we replaced the hydrophobic cinnamoyl moiety by the somewhat less hydrophobic Boc group.

In coronaviruses, nonstructural protein 5 (Nsp5) is the main protease (Mpro).Similar to the enteroviral 3Cpro, it is a cysteine protease in the vast majority of cases and has, therefore, also been called a ″3C-like protease” (3CLpro). The first crystal structure of a CoV Mpro or 3CLpro revealed that two of the three domains of the enzyme together resemble the chymotrypsinlike fold of the enteroviral 3Cpro, but there is an additional α-helical domain that is involved in the dimerization of the protease.In particular their almost absolute requirement for Gln in the P1 position of the substrate and space for only small amino-acid residues such as Gly, Ala, or Set in the P1′ position, encouraging us to explore the coronaviral Mpro and the enteroviral 3Cpro as a common target for the design of broad-spectrum antiviral compounds. The fact that there is no known human protease with a specificity for Gln at the cleavage site of the substrate increases the attractiveness of this viral target, as there is hope that the inhibitors to be developed will not show toxicity versus the host cell. Indeed, neither the enterovirus 3Cpro inhibitor rupintrivir, which was developed as a treatment of the common cold caused by HRV, nor the peptide aldehyde inhibitor of the coronavirus Mpro that was recently demonstrated to lead to complete recovery of cats from the normally fatal infection with Feline Infectious Peritonitis Virus (FIPV) showed any toxic effects on humans or cats,

respectively. We chose the chemical class of peptidomimetic α-ketoamides to assess the feasibility of achieving antiviral drugs targeting coronaviruses and enteroviruses with nearequipotency.

Here we describe the structure-based design, synthesis, and evaluation of the inhibitory activity of a series of compounds with broad-spectrum activities afforded by studying the structure−activity relationships mainly with respect to the P2 position of the peptidomimetics. One of the compounds designed and synthesized exhibits excellent activity against MERS-CoV.

MATERIALS AND METHODS

Compounds

GC373 and GC375 were synthesized as reported elsewhere. The aldehyde bisulfite adducts salt GC376 was synthesized as described in the supplemental material. The structures of the dipeptide inhibitors are shown in Rupintrivir, a protease inhibitor designed against HRV 3Cpro, was purchased from Axon Medchem (Groningen, Netherlands) and used as a control

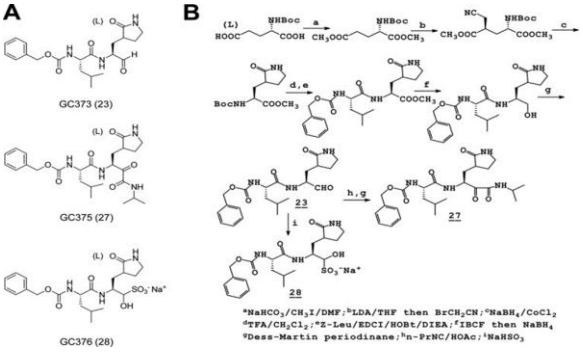

Figure -Structures (A) and summary of synthesis (B) of dipeptide inhibitors. GC373, GC375, and GC376

Various cell lines, including HG23, CRFK, RAW267.4, ST, CCL-9.1, MRC-5, FRhK-4, HeLa, and Vero cells, were maintained in Dulbecco's minimal essential medium (DMEM) or MEM containing 5% fetal bovine serum and antibiotics (chlortetracycline [25 μg/ml], penicillin [250 U/ml], and streptomycin [250 μg/ml]). All cells except for HG23 cells were obtained from ATCC (Manassas, VA). Viruses used in this study were FCV (strain Urbana), MNV-1, TGEV (strain Miller), BCV (a field isolate from the Kansas State University [KSU] diagnostic lab), FIPV (strain 1146), human coronavirus 229E, MHV (strain A59), HAV (strain HM175), PTV 51, and 68). FCV and MNV-1 were obtained from K. Green at the NIH and from H. Virgin at Washington University (St. Louis, MO), respectively. BCV and PTV were obtained from the KSU diagnostic lab. All other viruses were obtained from ATCC.

Expression and purification of 3Cpro and 3CLpro

The cDNAs encoding full-length viral 3Cpro or 3CLpro of TGEV and HAV were amplified by reverse transcription-PCR (RT-PCR) as previously described. Primers contained the nucleotide sequences of each corresponding protease, for cloning, as well as the nucleotides for 6 His residues (in the forward primers). The codon-optimized cDNAs for 3Cpro or 3CLpro of NV, MD145, SARS-CoV, PV, and FMDV were synthesized fused with 6 His at the N terminus

FRET protease Assay:

The fluorescence resonance energy transfer (FRET) protease assay was performed as follows. Stock solutions (10 mM) of the substrates and the compounds were prepared in dimethyl sulfoxide (DMSO) and diluted in assay buffer. The assay buffer comprised 20 mM HEPES buffer containing NaCl (0 mM for HAV 3Cpro and 200 mM for all other proteases), 0.4 mM EDTA, glycerol (60% for NV and MD145 3CLpro and 30% for TGEV and 229E 3CLpro), and 6 mM (NV and MD145 3CLpro and HAV 3Cpro) or 4 mM (all other proteases) dithiothreitol (DTT) at pH 6 (coronavirus 3CLpro) or 8 (all other proteases). Each protease was mixed with serial dilutions of each compound or with DMSO in 25 μl of assay buffer and incubated at 37°C for 30 min, followed by the addition of 25 μl of assay buffer containing substrate. Fluorescence readings were obtained using an excitation wavelength of 360 nm and an emission wavelength of 460 nm on a fluorescence microplate reader (FLx800; Biotek, Winooski, VT) 1 h following the addition of substrate. Relative fluorescence units (RFU) were determined by subtracting background values (substrate-containing well without protease) from the raw fluorescence values as described previously.

Table 1 Virus proteases and fluorogenic substrates used for FRET protease assaysa

Virus family and virus	Fluorogenic substrate	Source and/or reference for fluorogenic substrate	Buffer conditions[b]			
			pH	Glycerol (%)	DTT (mM)	NaCl (mM)
Caliciviridae						
NV	Edans-DFHLQ/GP-Dabcyl (truncated)	46	8	60	6	120
MD145	Edans-DFHLQ/GP-Dabcyl		8	60	6	120
Coronaviridae						
TGEV	Dabcyl-KTSAVLQ/SGFRKME-Edans	Bachem; 24	6	30	4	120
SARS-CoV	Dabcyl-KTSAVLQ/SGFRKME-Edans		6	30	4	120
Picornaviridae						
PV	Dabcyl-KTSAVLQ/SGFRKME-Edans		8	20	4	120
HRV	Edans-DFHLQ/GP-Dabcyl		7	20	4	120
HAV	Dabcyl-GLRTQ/SFS-Edans	Bachem	7	20	4	120
FMDV	Edans-APAKQ/LLN-Dabcyl	22	8	50	4	120

aNV, norovirus strain Norwalk; MD145, norovirus strain MD145; TGEV, transmissible gastroenteritis virus; SARS-CoV, severe acute respiratory syndrome coronavirus; PV, poliomyelitis virus; HRV, human rhinovirus; HAV, human hepatitis A virus; FMDV, foot-and-mouth disease virus.

bThe buffer contained 20 mM HEPES and 0.4 mM EDTA.

Cell-based inhibition assays.

The effects of each compound on viral replication were examined in cell culture systems. Virus-infected cells were incubated at 37°C, except for HRV-infected HeLa cells, which were maintained at 33°C. The viruses and corresponding cell lines are listed in Table 2. Briefly, confluent or semiconfluent cells were inoculated with virus at a multiplicity of infection of 0.05 for 1 h, and the inoculum was replaced with medium containing DMSO (<0.1%) or each compound (up to 100 μM). The virus-infected cells were further incubated for up to 168 h, and the replication of virus was measured by the 50% tissue culture infective dose (TCID50) method and/or real-time quantitative RT-PCR (qRT-PCR). The TCID50 method was used for titration of viruses showing apparent cell cytopathic effects, which included FCV, MNV-1, TGEV, FIPV, MHV, BCV, HAV, 229E, EV71, and PTV. Real-time qRT-PCR was performed for titration of NV (replicon-harboring cells) and HRV. For HAV and 229E, real-time qRT-PCR was also used to confirm the TCID50 results. For real-time qRT-PCR, RNA was extracted from each sample (cell lysates for HG23 cells and viral suspensions for HAV, HRV, and 229E) by use of an RNeasy kit (Qiagen, Valencia, CA), followed by amplification in a Cepheid SmartCycler with the following parameters: 45°C for 30 min and 95°C for 10 min followed by 40 cycles of denaturation at 95°C for 30 s, annealing at 50°C for 1 min, and elongation at 72°C for 30 s.

Table 2 Viruses and corresponding cell lines used in cell culture

Virus family	Virus[a]	Cell line
Caliciviridae	NV	HG23
	FCV	CRFK
	MNV-1	RAW267.4
Coronaviridae	TGEV	ST
	FIPV	CRFK
	229E	MRC-5
	MHV	CCL-9.1
	BCV	HRT-18

Virus family	Virus[a]	Cell line
Picornaviridae	HAV	FRhK-4
	EV71	Vero
	HRV 18, 51, and 68	HeLa
	PTV	ST

aMNV-1, murine norovirus 1; FIPV, feline infectious peritonitis virus; 229E, human coronavirus 229E; MHV, mouse hepatitis virus; BCV, bovine coronavirus; EV71, enterovirus 71; HRV 18, 51, and 68, human rhinovirus strains 18, 51, and 68; PTV, porcine teschovirus.

Nonspecific cytotoxic effects.

The toxic dose for 50% cell death (TD50) for each compound was determined for the various cells used in this study. Confluent cells grown in 96-well plates were treated with various concentrations (1 to 500 μM) of each compound for 72 h. Cell cytotoxicity was measured by a CytoTox 96 nonradioactive cytotoxicity assay kit and crystal violet staining. The in vitro therapeutic index was calculated by dividing the TD50 by the IC50.

X-ray crystallography: crystallization and data collection.

Details regarding crystallization, data collection, structure solution, and refinement are provided in Table S1 in the supplemental material. Briefly, all crystallization trials were conducted in high-throughput Compact sitting-drop vapor diffusion plates at 20°C, using equal volumes of protein and crystallization solution equilibrated against 75 μl of the latter. Crystals of apo-NV 3CLpro or an NV 3CLpro-, PV 3Cpro-, or TGEV 3CLpro-GC376

Photon Source beamline 17-ID, using a Dectris Pilatus 6 M pixel array detector. Structure solution was conducted by molecular replacement with Molrep and refinement and model building were carried out with Phenix and Coot , respectively.

Result

Structure-Based Design of α-Ketoamides. Our efforts to design novel α-ketoamides as broad-spectrum inhibitors of coronavirus Mpros and enterovirus 3Cpros started with a detailed analysis of the following crystal structures of unliganded target enzymes: SARS-CoV Mpro , bat coronavirus HKU4 Mpro as a surrogate for the closely related MERS-CoV protease, Coxsackievirus B3, 3Cpro; enterovirus D68 3Cpro and enterovirus A71 3Cpro .During the course of the present study, we determined crystal structures of a number of lead α-ketoamide compounds in complex with SARS-CoV Mpro, HCoV-NL63 Mpro, and CVB3 3Cpro, in support of the design of improvements in the next round of lead optimization. Notably, unexpected differences between alpha- and betacoronavirus Mpro were found in this study. The structural foundation of these was elucidated in detail in a subproject involving the Mpro of HCoV NL63; because of its volume, this work will be published separately and only some selected findings are referred to here. The main protease of the newly discovered coronavirus linked to the Wuhan outbreak of respiratory illness is 96% identical (98% similar) in the aminoacid sequence to that of SARS-CoV Mpro so all results reported here for the inhibition of SARS-CoV will most likely also apply to the newvirus.

As the proteases targeted in our study all specifically cleave the peptide bond following a P1-glutamine residue derivative of glutamine as the P1 residue in all our α-ketoamides . This moiety has been found to be a good mimic of glutamine and enhance the power of the inhibitors by up to 10-fold, most probably because, compared to the flexible glutamine side chain, the more rigid lactam leads to a reduction of the loss of entropy upon binding to the target protease. Our synthetic efforts were, therefore, aimed at opttimizing the substituents at the P1′, P2, and P3 positions of the α-ketoamides.

Synthesis of a-ketoamides

Synthesis started with the dianionic alkylation of NBoc glutamic acid dimethyl ester with bromoacetonitrile. As expected, this alkylation occurred in a highly stereoselective manner, giving 1 as the exclusive product.

- In the following step, the cyano group of 1 was subjected to hydrogenation
- The in-situ cyclization of the resulting intermediate afforded the lactam 2.
- The lactam derivative 3 was generated by removal of the protecting group of 2.
- On the other hand, the amidation of acyl chloride and a-amino acid methyl ester afforded the

intermediates 4, which gave rise to the acids 5 via alkaline hydrolysis.

- The key intermediates 6 were obtained via the condensation of the lactam derivative 3 and the N-capped amino acids 5.
- The ester group of compounds 6 was then reduced to the corresponding alcohol.
- Oxidation of the alcohol products 7 by Dess-Martin periodinane generated the aldehydes 8, which followed by nucleophilic addition with isocyanides gave rise to compounds 9 under acidic conditions.
- Then, the a-hydroxyamides 10 were prepared by removing the acetyl group of compounds 9.
- In the final step, the oxidation of the exposed alcohol group in compounds 10 generated our target a-ketoamides 11.
- The inhibitory potencies of candidate a-ketoamides were evaluated against purified recombinant

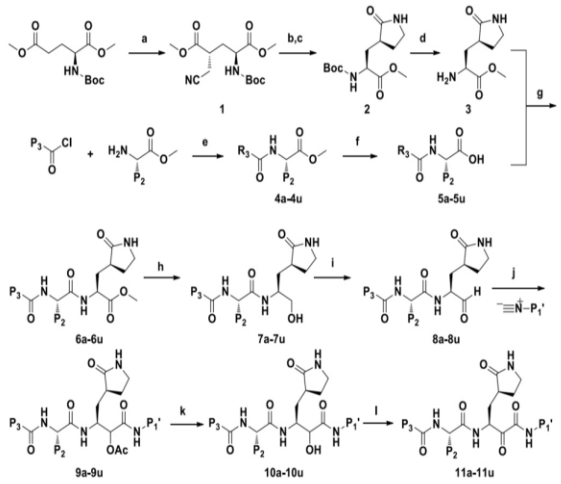

Viral replicons

To enable the rapid and biosafe screening of antivirals against corona- and enteroviruses, a non-infectious, but replication-competent SARS-CoV replicon was used33 along with subgenomic replicons of CVB334 and EV-A71. The easily detectable reporter activity (firefly or Renilla luciferase) of these replicons has previously been shown to reflect viral RNA synthesis.33-35 In-vitro RNA transcripts of the enteroviral replicons were also used for transfection. For the SARS-CoV replicon containing the CMV promoter, only the plasmid DNA was used for transfection.

Variation of the P1' and P3 substituents

P1' substituent

The crystal structures indicated that the fit of the P1' benzyl group of 11a in the S1' pocket might be improved. The amide oxygen of the warhead accepts an H-bond from the imidazole of His41 in the complexes with SARS-CoV Mpro and HCoV-NL63 Mpro, and from the oxyanion-hole amide of Gly145 in CVB3 3Cpro, but the P1' benzyl group appears not fully embedded in the pocket .We therefore replaced it by n-butyl in 11b . This resulted in an improvement of the inhibitory activity against CVB3 3Cpro (from IC50 = 6.6 to 1.0 µM), whereas that against the EV-A71 enzyme was somewhat weaker (IC50 = 2.4 µM). Most importantly, however, the compound proved totally inactive against recombinant SARS-CoV Mpro (IC50 > 50 µM). Replacement of the P1' substituent by tert-butyl in 11c led to very poor activities against all three proteases, and P1' = isobutyl (11d) or 2-methoxy-2-oxoethyl (11e) were not much better. Therefore,although there is probably room for further improvement, we decided to maintain the original design with P1' = benzyl.

P3 substituent

Inspection of the crystal structures of 11a in complex with SARS-CoV Mpro and CVB3 3Cpro suggested that the interaction of the P3-cinnamoyl group with the binding cleft might be sub-optimal. In order to furnish the P3 group with more flexibility, we reduced the double bond in 11a to generate 11g. However, presumably for entropic reasons, this led to a 2- to 3-fold decrease in activity against the SARS-CoV Mpro and the EV-A71 3Cpro, compared to compound 11a. CVB3 3Cpro was the only protease against which an improvement by the reduction of the double bond of the cinnamoyl group was noted, but in the replicon assays, compound 11g was inferior to 11a in all cases (Table S2).

Introduction in P3 of less flexible, bulky substituents such as 2,3-dihydrobenzo[b][1,4]dioxine-6-carbonyl (11h) and 2,3-dihydrobenzo[b][1,4]dioxine-5-carbonyl (11i) also met with limited success; IC50 values were mediocre for inhibition of the EV-A71 3Cpro and the CVB3 3Cpro and higher by a factor of at least 5 for inhibition of the SARS-CoV Mpro, compared to compound 11a. P3 = benzofuran-2-carbonyl (11j) led to a further reduction of inhibitory activity, particularly against the EV-A71 3Cpro.

Compounds with P3 = benzo[b]thiophene-2-carbonyl (11k) and 6-bromoimidazo[1,2-a]pyridine-2-carbonyl (11l) were inactive against EV-A71 3Cpro and only very moderately active against CVB3 3Cpro and SARS-CoV Mpro (Table S1). Inspection of the template crystal structures revealed that all of these substituents would occupy the space of the main chain of a peptide substrate at the S3 and partly S4 sites and are unable to reach into the space normally taken by a P3 amino-acid side-chain (which would be relatively unrestricted in all three proteases).However, in the predicted main-chain-like orientation, the extended aromatic groups would interfere with the NH group of Leu127 and the carbonyl of Gly164. In summary, the cinnamoyl group of the original compound, 11a, Was superior to all other substituents explored. Among the compounds tested thus far, 11a resulted in the best inhibitory activities towards both enterovirus 3Cpro and SARS-CoV Mpro.Accordingly, we decided to retain the cinnamoyl group as the substituent at the P3 position.

CONCLUSIONS

The viruses selected for evaluation in our study are important human and animal pathogens in the Caliciviridae, Coronaviridae, and Picornaviridae families. The Caliciviridae family includes 4 genera, namely, Vesivirus, Lagovirus, Norovirus, and Sapovirus. The NV and MD145 strains belong to norovirus genotypes I and II, respectively. Noroviruses of these genotypes are associated with the majority of norovirus outbreaks in humans.

This work demonstrates the power of structure-based approaches in the design of broad-spectrum antiviral compounds with roughly equipotent activity against coronaviruses and enteroviruses. We observed a good correlation between the inhibitory activity of the designed compounds against the isolated proteases, in viral replicons, and in virus-infected Huh7 cells. One of the compounds (11r) exhibits excellent anti-MERS-CoV activity in virus-infected Huh7 cells.Because of the high similarity between the main proteases of SARSCoV and the novel BetaCoV/Wuhan/2019; we expect 11r to exhibit good antiviral activity against the new coronavirus as well.

REFERENCE

[1] Hilgenfeld, R.; Peiris, M. From SARS to MERS: 10 years of research on highly pathogenic human coronaviruses. Antiviral Res.2013, 100, 286−295.(2) Zaki, A. M.; van Boheemen, S.; Bestebroer, T. M.; Osterhaus, A.D.; Fouchier, R. A. Isolation of a novel coronavirus from a man with pneumonia in Saudi Arabia. N. Engl. J. Med. 2012, 367, 1814−1820.

[2] Eckerle, I.; Muller, M. A.; Kallies, S.; Gotthardt, D. N.; Drosten,C. In-vitro renal epithelial cell infection reveals a viral kidney tropism as a potential mechanism for acute renal failure during Middle East Respiratory Syndrome (MERS) Coronavirus infection. Virol. J. 2013,10, 359.

[3] Butler, D. South Korean MERS outbreak spotlights lack of research. Nature 2015, 522, 139−140.

[4] Ge, X. Y.; Li, J. L.; Yang, X. L.; Chmura, A. A.; Zhu, G.; Epstein,J. H.; Mazet, J. K.; Hu, B.; Zhang, W.; Peng, C.; Zhang, Y. J.; Luo, C.M.; Tan, B.; Wang, N.; Zhu, Y.; Crameri, G.; Zhang, S. Y.; Wang, L.F.; Daszak, P.; Shi, Z. L. Isolation and characterization of a bat SARSlike coronavirus that uses the ACE2 receptor. Nature 2013, 503, 535−538.

[5] Menachery, V. D.; Yount, B. L., Jr.; Debbink, K.; Agnihothram,S.; Gralinski, L. E.; Plante, J. A.; Graham, R. L.; Scobey, T.; Ge, X. Y.;Donaldson, E. F.; Randell, S. H.; Lanzavecchia, A.; Marasco, W. A.;Shi, Z. L.; Baric, R. S. A SARS-like cluster of circulating bat coronaviruses shows potential for human emergence. Nat. Med. 2015,21, 1508−1513.

[6] Yang, X. L.; Hu, B.; Wang, B.; Wang, M. N.; Zhang, Q.; Zhang,W.; Wu, L. J.; Ge, X. Y.; Zhang, Y. Z.; Daszak, P.; Wang, L. F.; Shi, Z.L. Isolation and characterization of a novel bat coronavirus closely related to the direct progenitor of severe acute respiratory syndrome coronavirus. J. Virol. 2016, 90, 3253−3256.

[7] Hu, B.; Zeng, L. P.; Yang, X. L.; Ge, X. Y.; Zhang, W.; Li, B.; Xie,J. Z.; Shen, X. R.; Zhang, Y. Z.; Wang, N.; Luo, D. S.; Zheng, X. S.;Wang, M. N.; Daszak, P.; Wang, L. F.; Cui, J.; Shi, Z. L. Discovery of a rich gene pool of bat SARS-related coronaviruses provides new insights into the origin of SARS coronavirus. PLoS Pathog. 2017, 13,No. e1006698.

[8] van der Hoek, L.; Pyrc, K.; Jebbink, M. F.; Vermeulen-Oost, W.;Berkhout, R. J.; Wolthers, K. C.; Wertheim-van Dillen, P. M.;Kaandorp, J.; Spaargaren, J.; Berkhout, B. Identification of a newhuman coronavirus. Nat. Med. 2004, 10, 368−373.

[9] Hamre, D.; Procknow, J. J. A new virus isolated from the human respiratory tract. Exp. Biol. Med. 1966, 121, 190−193.

[10] da Silva Filho, L. V.; Zerbinati, R. M.; Tateno, A. F.; Boas, L.V.; de Almeida, M. B.; Levi, J. E.; Drexler, J. F.; Drosten, C.; Pannuti,C. S. The differential clinical impact of human coronavirus species in children with cystic fibrosis. J. Infect. Dis. 2012, 206, 384−388.

[11] Mayer, K.; Nellessen, C.; Hahn-Ast, C.; Schumacher, M.;Pietzonka, S.; Eis-Hubinger, A. M.; Drosten, C.; Brossart, P.; Wolf, D.Fatal outcome of human coronavirus NL63 infection despite successful viral elimination by IFN-alpha in a patient with newly diagnosed ALL. Eur. J. Haematol. 2016, 97, 208−210.

[12] Lee, J.; Storch, G. A. Characterization of human coronavirus OC43 and human coronavirus NL63 infections among hospitalized children < 5 years of age. Pediatr. Infect. Dis. J. 2014, 33, 814−820.

[13] Oermann, C. M.; Schuster, J. E.; Conners, G. P.; Newland, J.G.; Selvarangan, R.; Jackson, M. A. Enterovirus D68. A focused review and clinical highlights from the 2014 U.S. outbreak. Ann. Am. Thorac.Soc. 2015, 12, 775−781.

[14] Xing, W.; Liao, Q.; Viboud, C.; Zhang, J.; Sun, J.; Wu, J. T.;Chang, Z.; Liu, F.; Fang, V. J.; Zheng, Y.; Cowling, B. J.; Varma, J. K.;Farrar, J. J.; Leung, G. M.; Yu, H. Hand, foot, and mouth disease in China, 2008−12: an epidemiological study. Lancet Infect. Dis. 2014,14, 308−318.

[15] Massilamany, C.; Gangaplara, A.; Reddy, J. Intricacies of cardiac damage in coxsackievirus B3 infection: implications for therapy. Int. J. Cardiol. 2014, 177, 330−339